COPII–Golgi protein interactions regulate COPII coat assembly and Golgi size

Yusong Guo and Adam D. Linstedt

Department of Biological Sciences, Carnegie Mellon University, Pittsburgh, PA 15213

Under experimental conditions, the Golgi apparatus can undergo de novo biogenesis from the endoplasmic reticulum (ER), involving a rapid phase of growth followed by a return to steady state, but the mechanisms that control growth are unknown. Quantification of coat protein complex (COP) II assembly revealed a dramatic up-regulation at exit sites driven by increased levels of Golgi proteins in the ER. Analysis in a permeabilized cell assay indicated that up-regulation of COPII assembly occurred in the absence GTP hydrolysis and any cytosolic factors other than the COPII prebudding complex Sar1p–Sec23p–Sec24p. Remarkably, acting via a direct interaction with Sar1p, increased expression of the Golgi enzyme *N*-acetylgalactosaminyl transferase-2 induced increased COPII assembly on the ER and an overall increase in the size of the Golgi apparatus. These results suggest that direct interactions between Golgi proteins exiting the ER and COPII components regulate ER exit, providing a variable exit rate mechanism that ensures homeostasis of the Golgi apparatus.

Introduction

Endomembrane compartments create specialized environments that are optimized for diverse reactions, including protein folding, quality control, processing, sorting, and turnover. How these compartments are established and maintained is a question of fundamental importance. Compartment size is somehow coupled to cell growth such that it increases as cells grow and remains roughly constant in postmitotic cells. On the other hand, during mitosis or differentiation, or in response to stress, secretory compartments can undergo extensive up- or down-regulation depending on cell type, developmental timing, or stress condition (Knaapen et al., 1997; Lee and Linstedt, 1999; Lu et al., 2001; Colanzi et al., 2003; Yu et al., 2003). Thus, homeostatic mechanisms that maintain a proper balance of membrane input and output at each compartment must be sufficiently flexible to allow extensive, rapid, and reversible changes.

Although signaling pathways, transcriptional events, and other higher order processes undoubtedly participate (Buccione et al., 1996; Ikonomov et al., 2001), compartment homeostasis might fundamentally rely on intrinsic features of the vesicle coat machinery. Transport vesicles typically fuse shortly after their formation, indicating that vesicle formation is rate limiting. Thus, the net flux of membrane through the Golgi apparatus, for example, would be determined by the rates at which vesicle coats acting at the ER and endosomes contribute input of vesicles and the rates at which vesicle coats acting at the Golgi drive vesicle export. What, then, determines the rate of vesicle production?

Assembly of the coat protein complex (COP) II coat on the ER membrane is initiated by guanine nucleotide exchange of the GTPase Sar1p (Futai et al., 2004). The presence of Sar1p-GTP leads to the successive recruitment of the coat components Sec23p–Sec24p and Sec13p–Sec31p (Matsuoka et al., 1998). COPII coat assembly is opposed by GTP hydrolysis by Sar1p triggered by Sec23p GAP activity and amplified by the presence of Sec13p–Sec31p (Yoshihisa et al., 1993; Antonny et al., 2001). Although each step may play a regulatory role that influences the rate of vesicle production, the self-terminating property of COPII assembly suggests that additional factors stabilize the coat on the membrane and regulate overall rate. Evidence suggests that cargo molecules in the ER membrane contribute (Aridor and Traub, 2002; Forster et al., 2006; Sato and Nakano, 2005). For example, synchronized export of vesicular stomatitus virus G protein (VSVG) stimulates COPII vesicle budding, and inhibition of protein synthesis depresses it (Aridor et al., 1999).

If compartment homeostasis is determined by vesicle production rates and vesicle production rates are influenced by cargo concentration, then it is important to ask whether

Correspondence to Adam D. Linstedt: linstedt@andrew.cmu.edu

Abbreviations used in this paper: BFA, brefeldin A; COP, coat protein complex; GalNAcT2, *N*-acetylgalactosaminyl transferase-2; NRK, normal rat kidney; VSVG, vesicular stomatitus virus G protein; VTC, vesicular-tubular cluster.

The online version of this article contains supplemental material.

The Journal of Cell Biology, Vol. 174, No. 1, July 3, 2006 53–63
http://www.jcb.org/cgi/doi/10.1083/jcb.200604058

compartment size is a function of cargo abundance. Here, we test the hypothesis that Golgi residents, in the guise of cargo at the ER, influence the size of the Golgi apparatus by regulating COPII assembly and thereby determining the extent of membrane input to the Golgi.

Results

Osmotic stress causes Golgi collapse and dispersal of Golgi components in the ER; yet, after cell volume recovery, the Golgi apparatus completely reassembles (Lee and Linstedt, 1999). Biogenesis of the Golgi apparatus from the ER is recapitulated using drug washout after sequential treatment with brefeldin A (BFA), to inhibit Arf1, and H89, to block COPII assembly. That is, the Golgi apparatus efficiently and synchronously reassembles from the ER (Puri and Linstedt, 2003). Inhibitor reversal is rapid, as indicated by restoration of membrane recruitment of Sec13 and β-COP at the earliest time points tested (Puri and Linstedt, 2003). During biogenesis, Golgi growth is rapid until steady state is reestablished, implying a temporary shift in the input/output balance at the Golgi that favors input.

To test the involvement of increased COPII assembly, we used morphological assays to determine the levels of COPII and Golgi assembly in cells before and during BFA/H89 washout. In normal rat kidney (NRK) cells, the Golgi marker giantin yielded the expected juxtanuclear ribbon structure before treatment, a dispersed ER pattern upon BFA/H89 treatment, and, during washout, a punctate vesicular-tubular cluster (VTC) pattern followed by reestablishment of the juxtanuclear Golgi ribbon (Fig. 1, A–D). In the same cells, staining of the COPII component Sec13 was restricted to ER exit sites before treatment, absent during treatment, and reestablished at exit sites during washout (Fig. 1, E–H). Significantly, quantification (see Materials and methods) revealed a reproducible peak of COPII assembly (Fig. 1 I). The transient up-regulation of COPII assembly was threefold ($P = 0.006$) greater than steady-state levels and coincided with the rapid phase of giantin emergence from the ER. HeLa cells, which exhibit significantly slower Golgi assembly (Puri and Linstedt, 2003), also yielded a peak in COPII assembly (twofold; $P = 0.01$), and this coincided in time with the delayed emergence of giantin from the ER, thereby confirming COPII up-regulation and its correlation with Golgi exit from the ER. Further, single HeLa cells expressing Sec13-GFP (Hammond and Glick, 2000) and imaged live at consecutive 2-min intervals while undergoing Golgi assembly during BFA/H89 washout also exhibited transient up-regulation in COPII assembly (Fig. 1 J). In contrast, untreated control cells exhibited relatively stable levels of COPII assembly (Fig. 1 J). In sum, a transient up-regulation in COPII assembly occurs during de novo biogenesis of the Golgi from the ER and coincides with Golgi egress marked by giantin.

The values shown represent, on a per-cell basis, the total above-threshold Sec13 fluorescence, which is a composite of

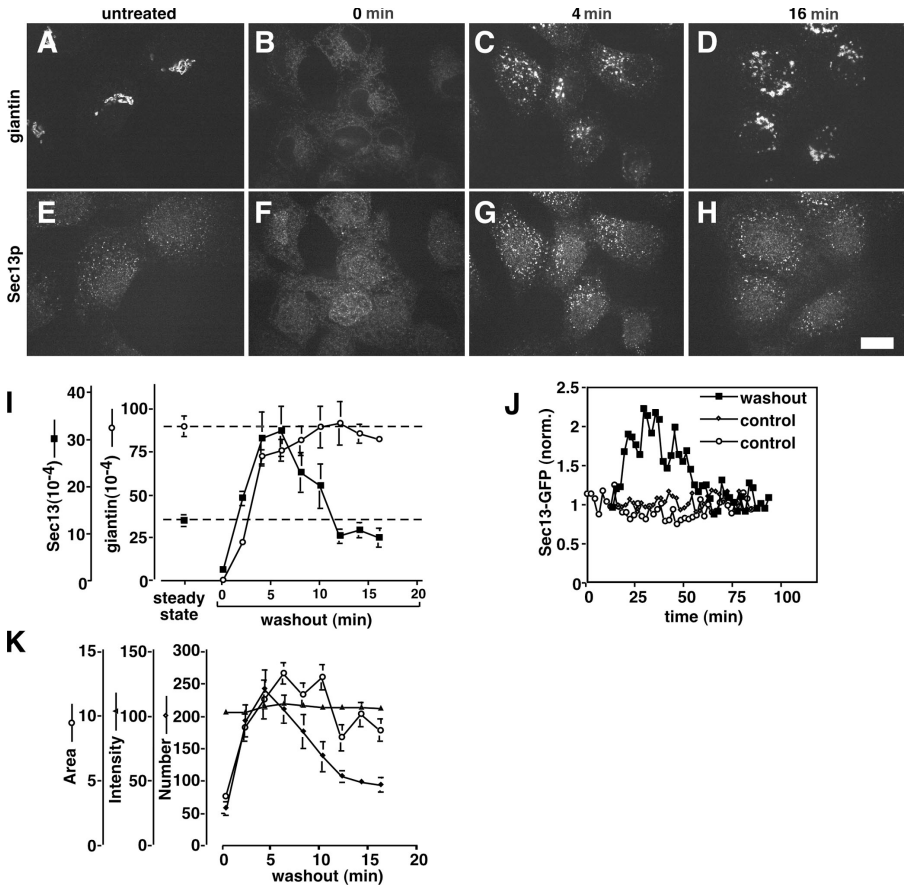

Figure 1. **Golgi biogenesis coincides with increased COPII assembly.** (A–H) NRK cells were untreated (A and E) or treated with BFA/H89 (30 min BFA and 10 min H89) followed by the indicated times of washout to allow Golgi assembly. The methanol-fixed cells were costained with anti-giantin (A–D) and anti-Sec13 antibodies (E–H). Single optical sections are shown. Bar, 10 μm. (I) To quantify COPII assembly and ER exit of giantin over time, total above-threshold fluorescence levels of Sec13 and giantin per NRK cell were determined (mean ± SEM; >15 cells each). Coincident with giantin exit, COPII assembly increased before returning to steady-state levels for untreated cells (dashed lines). (J) Quantified COPII assembly based on GFP-Sec13 expression in HeLa cells is compared for a representative cell after BFA/H89 washout and two untreated control cells. Imaging was at 2-min intervals, and values are corrected and normalized to adjust for slight photobleaching and to allow direct comparison. (K) Means per cell for the number, area, and intensity of above-threshold Sec13 objects are compared over time during BFA + H89 washout in NRK cells. Note that increases in exit sites, i.e., object number, and mean size account for the total COPII assembly increase shown in I.

the number of exit sites per cell, their size, and their intensity. Analysis of these parameters indicated that the change in total fluorescence was due to both increased size of exit sites and change in number (Fig. 1 K). Thus, up-regulation during Golgi biogenesis involves up-regulated assembly at preexisting sites as well as the formation of new ER exit sites.

ER-localized Golgi proteins may activate COPII recruitment at new and preexisting sites. As a test, we used BFA treatment to induce redistribution of Golgi enzymes to the ER. Unlike the combined BFA/H89 treatment, BFA alone, which inhibits Arf1 guanine nucleotide exchange factor (Donaldson et al., 1992; Helms and Rothman, 1992), does not prevent COPII assembly (Orci et al., 1993; Bednarek et al., 1995; Ward et al., 2001). Indeed, in BFA-treated NRK cells, Sec13 remained localized to exit sites, whereas the Golgi enzyme mannosidase II was dispersed in the ER (unpublished data). Importantly, Sec13 staining increased to a new, higher steady state (twofold; $P = 0.002$) during BFA treatment (Fig. 2 A) and, during washout, returned to its original steady-state levels (Fig. 2 B). The increase was due to both increased exit site size (1.7-fold; $P = 0.02$) and the formation of new sites (1.3-fold; $P = 0.0008$). BFA-induced twofold up-regulation of COPII assembly involving preexisting and new sites was also observed in single cells using live imaging of Sec13-GFP (Fig. S1, available at http://www.jcb.org/cgi/content/full/jcb.200604058/DC1). Presumably, Golgi proteins induce COPII up-regulation while undergoing ER exit that, in the presence of BFA, is sustained because of the immediate recycling of Golgi enzymes back to the ER (Ward et al., 2001; Puri and Linstedt, 2003).

These results suggest that the Golgi protein expression level might influence COPII assembly. Therefore, the level of Sec13 at exit sites was determined in a HeLa cell line stably overexpressing the Golgi enzyme *N*-acetylgalactosaminyl transferase-2 (GalNAcT2) coupled to GFP (T2-GFP). In overexpressing cells, T2-GFP was readily detected in both the Golgi and the ER (see Fig. 7 D). The cell line also contained cells expressing little or no T2-GFP, and these cells provided an internal control sample. Strikingly, relative to these control cells, overexpressors exhibited increased levels (1.7-fold; $P = 0.006$) of Sec13 staining at exit sites (Fig. 2 C). Altogether, these results indicate that increased Golgi protein abundance in the ER triggers increased COPII assembly through new exit site formation and that, if sustained, even for a single Golgi protein, a new steady-state level is established.

To address the mechanism of stimulated COPII recruitment by ER-localized Golgi proteins, we used a permeabilized cell assay in which COPII assembly is performed on salt-washed cells in the presence of nonhydrolysable GTP (Lee and Linstedt, 2000). One possibility is that ER-localized Golgi proteins, either directly or indirectly, inhibit GTP hydrolysis by the Sar1 GTPase. For the COPI coat, such a mechanism might stabilize the coat on the membrane, thereby ensuring productive, i.e., cargo-loaded, vesicle formation (Goldberg, 2000). If enhanced COPII recruitment by ER-localized Golgi components depends on inhibition of GTP hydrolysis, then nonhydrolysable GTP should negate the difference in COPII assembly between control and BFA-treated or T2-GFP–overexpressing cells. However, despite the presence of GTPγS, BFA-treated cells exhibited twofold-increased COPII recruitment, as detected by Sec13 staining at exit sites (Fig. 3, A and B) and by Sec13 immunoblotting (Fig. 3 D). As expected, the assay itself was cytosol dependent, and enhanced Sec13 recovery was evident at all cytosol concentrations tested (Fig. 3 C). A cytosol-dependent and statistically significant increase in COPII recruitment was also observed in the presence of GTPγS in permeabilized cells overexpressing T2-GFP (see Fig. 6; unpublished data). Assembly increase in the absence of GTP hydrolysis argues against a mechanism involving inhibition of Sar1-GTP hydrolysis. This conclusion is consistent with a direct measurement showing a slight elevation, rather than inhibition, of GTP hydrolysis by Sar1p in the presence of the yeast cargo receptor Emp47p (Sato and Nakano, 2005).

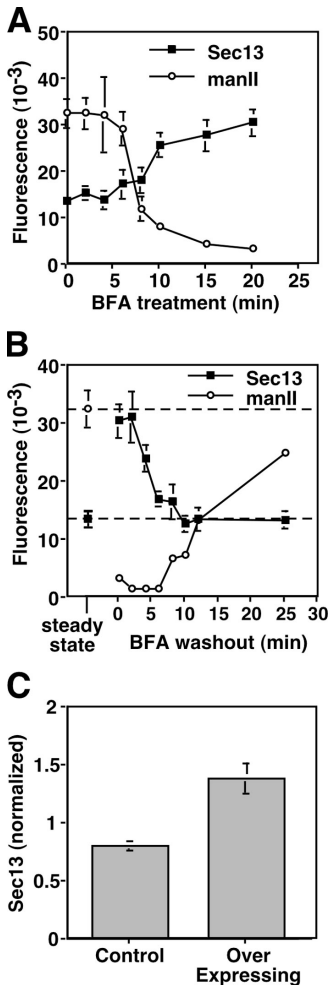

Figure 2. **ER-localized Golgi proteins up-regulate COPII assembly.** (A and B) At various times of BFA treatment (A) and washout (B), methanol-fixed NRK cells were analyzed for COPII assembly and post-ER mannosidase II (manII; mean ± SEM; >15 cells each). COPII assembly increased upon BFA-induced ER localization of Golgi enzymes and returned to the steady-state level of untreated cells (dashed lines) upon Golgi enzyme exit. (C) COPII assembly was quantified in paraformaldehyde-fixed and Sec13-stained HeLa cells stably expressing T2-GFP. Control cells were those that expressed little or no detectable T2-GFP, whereas overexpressing cells yielded strong Golgi staining and detectable ER staining. Values are normalized means ± SEM ($n = 4$; >25 cells each).

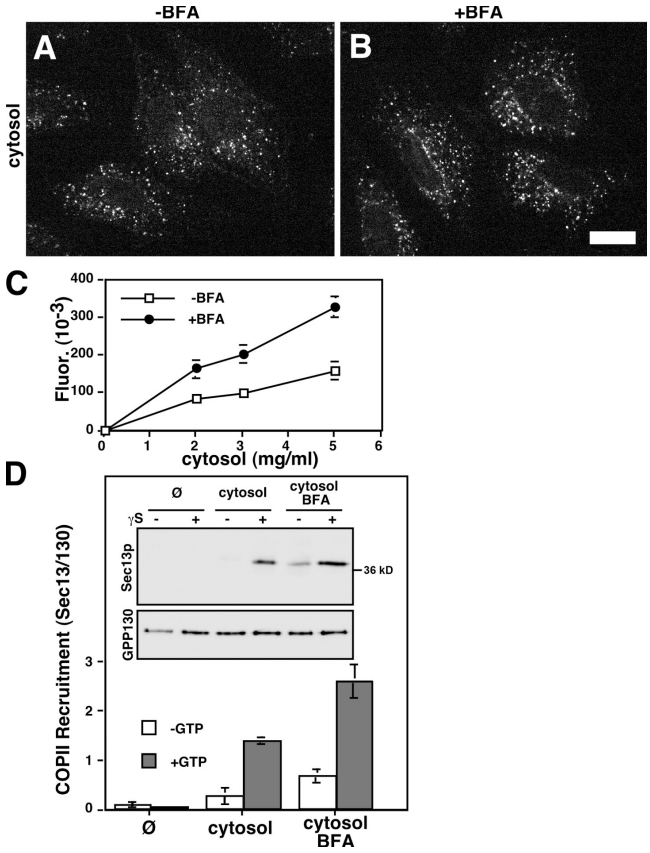

Figure 3. **Increased COPII assembly occurs in the absence of GTP hydrolysis.** (A and B) A permeabilized cell COPII assembly assay was performed on untreated (A) and BFA-treated (B) NRK cells. Reactions contained ATP, GTPγS, and 2 mg/ml cytosol. Images are single optical sections of paraformaldehyde-fixed cells showing Sec13 localization. Bar, 10 μm. (C) Quantification of Sec13 at exit sites indicated that, despite the presence of GTPγS, BFA-treated cells exhibited increased COPII assembly at the indicated cytosol concentrations (mean ± SEM; >15 cells each). (D) The permeabilized assay was also quantified by immunoblotting. Recovery of Sec13 and a loading control, the Golgi membrane protein GPP130, are shown for untreated or BFA-treated cells after incubation in buffer (Ø) or 4 mg/ml cytosol. Absence or presence of GTPγS is also indicated. Quantification of the Sec13/GPP130 ratio confirmed that COPII assembly was similarly increased by BFA despite the presence of GTPγS (mean ± SEM; $n = 3$).

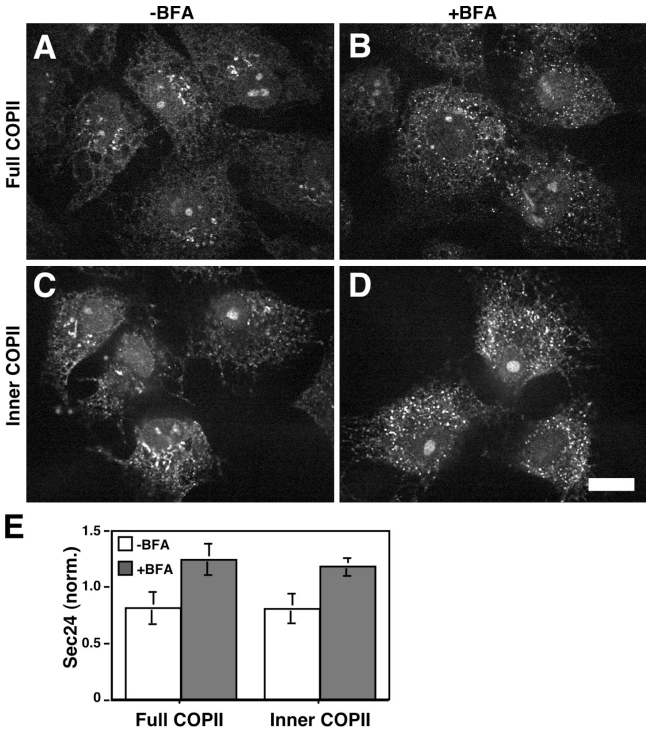

Figure 4. **Purified COPII is sufficient for increased assembly.** (A–D) A permeabilized cell COPII assembly assay was performed on untreated (A and C) and BFA-treated (B and D) NRK cells. Reactions contained ATP and GTPγS and either the full COPII components Sar1p, Sec24p–Sec23p, and Sec13p–Sec31p (A and B) or just the inner COPII components Sar1p and Sec24p–Sec23p (C and D). Images are single optical sections of paraformaldehyde-fixed cells showing Sec24p localization. Bar, 10 μm. (E) Quantified results based on Sec24p staining of untreated and BFA-treated permeabilized NRK cells are compared for COPII assembly using the full COPII components Sar1p, Sec24p–Sec23p, and Sec13p–Sec31p or the inner COPII components Sar1p and Sec24p–Sec23p (normalized mean ± SEM; >15 cells each).

To determine whether COPII components alone are sufficient for up-regulated COPII assembly, the permeabilized cell assay was performed using purified COPII in place of cytosol. Yeast COPII was chosen as a convenient source that has previously been shown to recapitulate aspects of assembly at exit sites in NRK cells (Kapetanovich et al., 2005). Consistent with previous work, purified COPII yielded assembly both in the juxtanuclear region and at peripheral exit sites, as detected by anti-Sec24p antibody staining after addition of Sar1p, Sec23p–Sec24p, and Sec13p–Sec31p (Fig. 4, A and E). Significantly, the signal was enhanced in BFA-treated cells relative to controls, indicating that purified COPII is sufficient to yield up-regulated COPII assembly (Fig. 4, B and E). Furthermore, when assembly and detection using anti-Sec24p antibodies were performed under identical conditions, except that Sec13p–Sec31p was omitted, up-regulated assembly was again observed (Fig. 4, C–E). Because Sar1p, Sec23p, and Sec24p form a prebudding complex in the absence of Sec13p and Sec31p (Aridor et al., 1998; Kuehn et al., 1998), these results indicate that increased COPII assembly occurs at the level of the prebudding complex. Thus, the mechanism of increased COPII assembly stimulated by ER-localized Golgi proteins occurs in the absence of any additional cytoplasmic factors or GTP hydrolysis and requires only the inner COPII components.

Based on these results, we considered the possibility that Sar1p alone might show increased binding. Indeed, although Sar1p yielded a diffuse ER localization rather than accumulation at exit sites (unpublished data), its membrane association was significantly increased in BFA-treated cells (Fig. 5 A). This suggests that Golgi components stimulate increased COPII assembly by promoting Sar1p binding possibly via direct interactions, as several Golgi proteins contain cytoplasmic domain dibasic motifs that interact with Sar1p and mediate their ER exit (Giraudo and Maccioni, 2003). As a test, we first determined whether the GalNAcT2 cytoplasmic domain, which contains a cluster of basic residues, binds purified Sar1p. An immobilized peptide corresponding to the GalNAcT2 cytoplasmic domain yielded robust and specific binding to Sar1p, whereas alanine substitution of the basic residues blocked binding (Fig. 5 B).

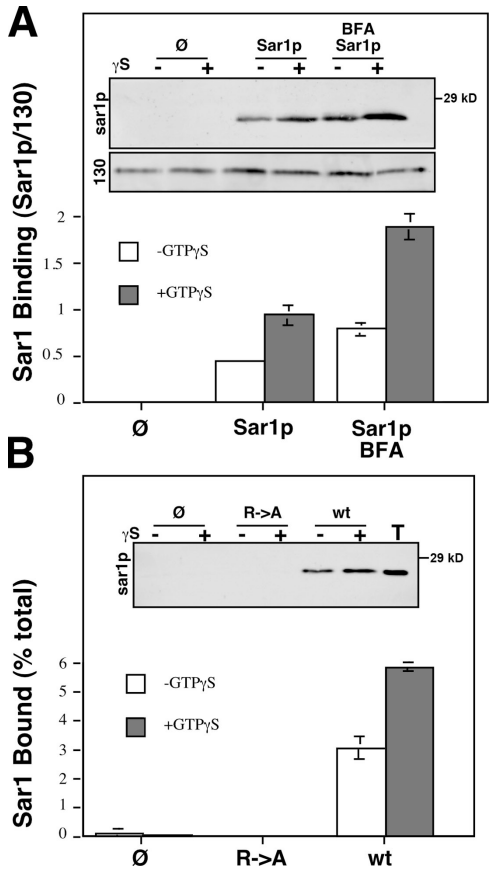

Figure 5. **Purified Sar1p shows enhanced recruitment and binds GalNAcT2.** (A) Untreated or BFA-treated permeabilized NRK cells were incubated without or with Sar1p in absence or presence of GTPγS. Recovery of membrane bound Sar1p and the loading control GPP130 was determined by immunoblotting. The quantified result, showing enhanced Sar1p binding to cells with ER-localized Golgi enzymes, is the ratio of Sar1p/GPP130 at each condition (mean ± SD; $n = 2$). (B) Purified Sar1p was tested for binding to the cytoplasmic domain peptide of GalNAcT2 (wild type [wt] = MRRRSRC) or a version with alanine substituted for arginine (R→A = MAAASAC). After incubation in the presence or absence of GTPγS, recovery of Sar1p bound to unconjugated (Ø) or peptide-conjugated thiopropyl Sepharose 6B beads was determined by immunoblotting. Each reaction contained 0.5 μg Sar1p, and 10% of this was also analyzed (T). The quantified results showing the percentage bound indicate a specific interaction (mean ± SD; $n = 2$).

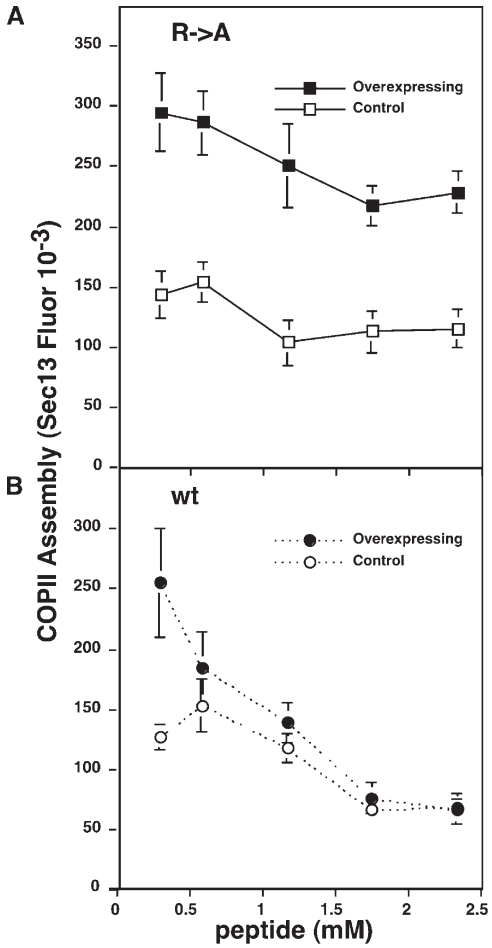

Figure 6. **Binding of Sar1p to GalNAcT2 underlies assembly increase.** (A and B) Permeabilized HeLa cells stably expressing GFP-T2 were incubated with GTPγS and 4 mg/ml cytosol containing the indicated concentration of R→A, the alanine-substituted peptide (A), or wt, the wild-type GalNAcT2 cytoplasmic domain peptide (B). COPII assembly, based on Sec13, was then quantified in T2-GFP–overexpressing cells and adjacent non- or low-expressing cells (mean ± SEM; >20 cells each). Representative images are presented in Fig. S2 (available at http://www.jcb.org/cgi/content/full/jcb.200604058/DC1). In contrast to the control, the GalNAcT2 peptide blocked the enhanced COPII assembly induced by GFP-T2 overexpression.

Binding occurred in the absence of added GTP but was enhanced by the presence of GTPγS. Thus, GalNAcT2 is capable of directly binding Sar1p, and it may stabilize Sar1p on the ER membrane, leading to enhanced COPII assembly.

Next, we asked whether presence of the GalNAcT2 cytoplasmic domain peptide would inhibit up-regulation of COPII assembly in cells overexpressing T2-GFP. Increasing concentrations of the alanine-substituted control peptide and GalNAcT2 cytoplasmic domain peptide were added together with cytosol and GTPγS to salt-washed permeabilized cells, and T2-GFP and Sec13 levels were determined (images presented in Fig. S2, available at http://www.jcb.org/cgi/content/full/jcb.200604058/DC1). As expected, cells overexpressing T2-GFP yielded increased COPII assembly compared with adjacent low expressors and the alanine-substituted control peptide (R→A) exerted little or no effect (Fig. 6 A). In contrast, the GalNAcT2 peptide potently inhibited the COPII assembly up-regulation triggered by T2-GFP overexpression (Fig. 6 B). A moderate inhibition of basal COPII assembly was also observed at higher peptide concentrations, indicating the involvement of the Sar1p dibasic binding site in COPII recruitment generally. Analysis of the area and number of Sec13-labeled exit sites per cell indicated that inhibition occurred at both up-regulated, preexisting sites and at newly formed exit sites (Fig. S3). In conclusion, increased T2-GFP in the ER stimulates new COPII assembly via direct binding to Sar1p. This offers an important variation on recent work showing stabilization of Sec23p–Sec24p membrane contact by cargo in the presence of multiple rounds of GTP hydrolysis by Sar1p (Sato and Nakano, 2005; Forster et al., 2006).

Further, these results reveal an elegant solution to the problem of transiently accelerated Golgi growth in the biogenesis assay. Increased availability of Golgi proteins in the ER stimulates COPII assembly via direct interaction with the coat,

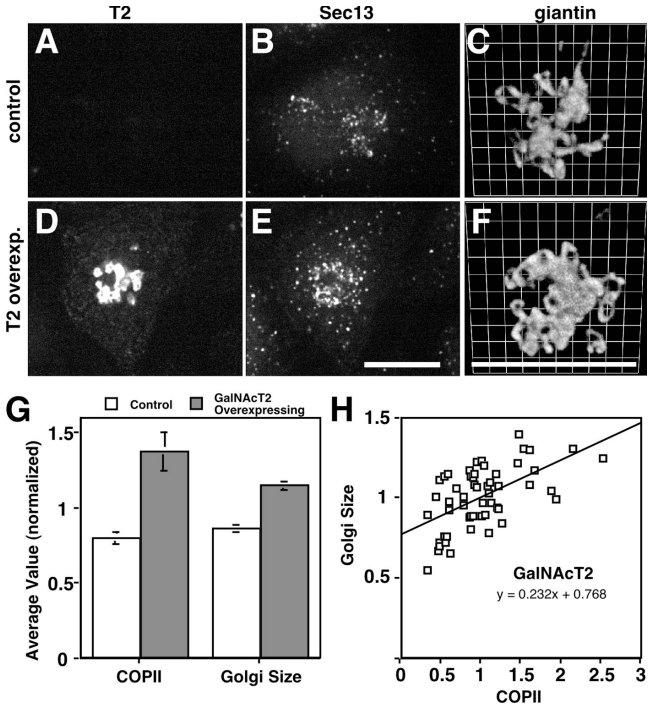

Figure 7. **GalNAcT2 up-regulates COPII assembly and Golgi size.** (A–F) Stable HeLa cell lines expressing T2-GFP were paraformaldehyde-fixed and analyzed to reveal GFP fluorescence (A and D) and Sec13 staining (B and E), each shown as Z axis projections of optical sections, as well as giantin staining (C and F) shown after 3D rendering. Control cells were those that expressed little or no detectable expression, whereas T2-GFP–overexpressing cells yielded strong Golgi and detectable ER staining. Bars, 10 μm. (G) COPII assembly and Golgi size were quantified for control and overexpressing T2-GFP cells. Values are normalized means (± SEM; $n = 4$; >25 cells each). Golgi size was total volume occupied by above-threshold fluorescence of giantin divided by apparent cell volume and showed a significant increase in T2-GFP–overexpressing cells. (H) COPII assembly level and the Golgi/cell size ratio were also compared on a cell-by-cell basis for single experiments. The correlation plot yielded a slope of 0.2.

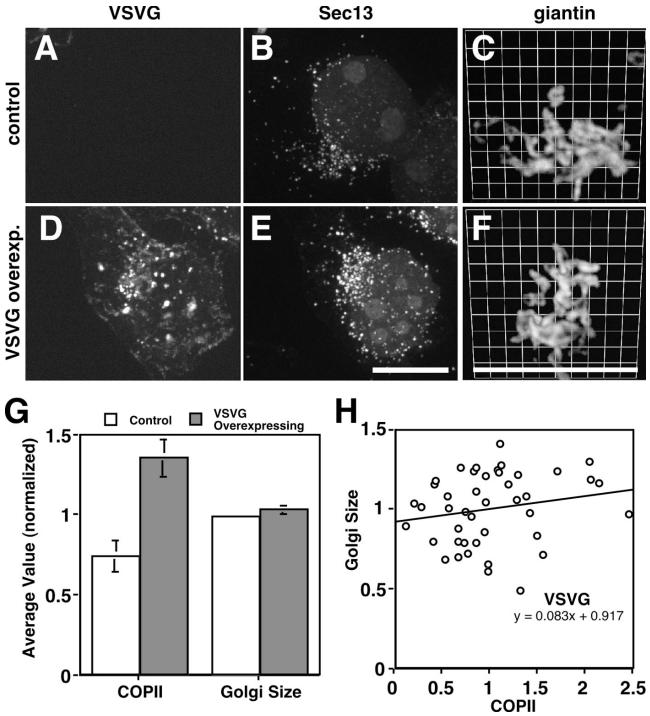

Figure 8. **VSVG up-regulates COPII assembly but not Golgi size.** (A–F) Stable HeLa cell lines expressing VSVG-GFP were paraformaldehyde-fixed and analyzed to reveal GFP fluorescence (A and D) and Sec13 staining (B and E), each shown as Z axis projections of optical sections, as well as giantin staining (C and F) shown after 3D rendering. In contrast to control cells, VSVG-GFP–overexpressing cells yielded strong apparent ER and surface staining. Bar, 10 μm. (G) COPII assembly and Golgi size were quantified for control and overexpressing VSVG-GFP (G) cells. Values are normalized means (± SEM; $n = 4$; >25 cells each). Although COPII assembly increased in VSVG-GFP–expressing cells, Golgi size did not. (H) COPII assembly level and the Golgi/cell size ratio were also compared on a cell-by-cell basis for single experiments. The correlation plot yielded a slope of only 0.08.

thereby favoring membrane input to the Golgi and Golgi growth. As ER levels of Golgi proteins subside, so does the rate of growth. Such a mechanism (hereafter referred to as variable coat assembly) may participate generally in Golgi homeostasis. That is, Golgi size may be determined by Golgi resident proteins regulating coat assembly at sites, such as ER, that directly impact the net Golgi input/output ratio. To test this, the size of the Golgi apparatus was quantified in cells exhibiting COPII up-regulation because of T2-GFP overexpression and compared with cells in the control sample. To estimate Golgi size, 3D confocal image sets were used to determine the volume of the staining corresponding to the Golgi marker giantin, as opposed to its staining intensity, and this value was normalized using total cell volume. Volume normalization reduced the variation due to normal Golgi growth and did not alter the experimental outcome. Strikingly, T2-GFP overexpressors exhibited up-regulated COPII assembly and yielded a mean normalized Golgi size that was 1.3-fold higher than control cells (Fig. 7, A–G). Note that giantin expression level, as determined by immunoblotting, was not altered by T2-GFP overexpression and that an identical apparent Golgi size increase was observed when the same analysis was performed using GM130 staining rather than giantin to determine Golgi size (1.3 ± 0.1 times greater in T2-GFP overexpressors). Further, the effect was not restricted to T2-GFP expression because both COPII assembly and Golgi size were also up-regulated in stable cells overexpressing GPP130-GFP (Fig. S4 A, available at http://www.jcb.org/cgi/content/full/jcb.200604058/DC1), a Golgi protein that, similar to GalNAcT2, contains cytoplasmic dibasic motifs (Linstedt et al., 1997). These findings, which report normalized means derived from multiple experiments, were further supported when the data was analyzed on a cell-by-cell basis for single experiments using a correlation matrix. As shown for T2-GFP overexpression, when the Sec13 level at exit sites was plotted against the ratio of Golgi/cell size, it was clear that increased COPII was associated with increased Golgi size (Fig. 7 H).

As controls for this experiment, Golgi size was determined upon overexpression of non-Golgi residents. First, we analyzed a stably transfected HeLa cell line expressing ts045-VSVG tagged with GFP (VSVG-GFP) at 37°C, a temperature that allows its trafficking to the cell surface. VSVG binds the COPII coat through a diacidic motif (Nishimura and Balch, 1997; Aridor et al., 1998), and synchronized movement of VSVG out of ER increases COPII vesicle production (Aridor et al., 1999).

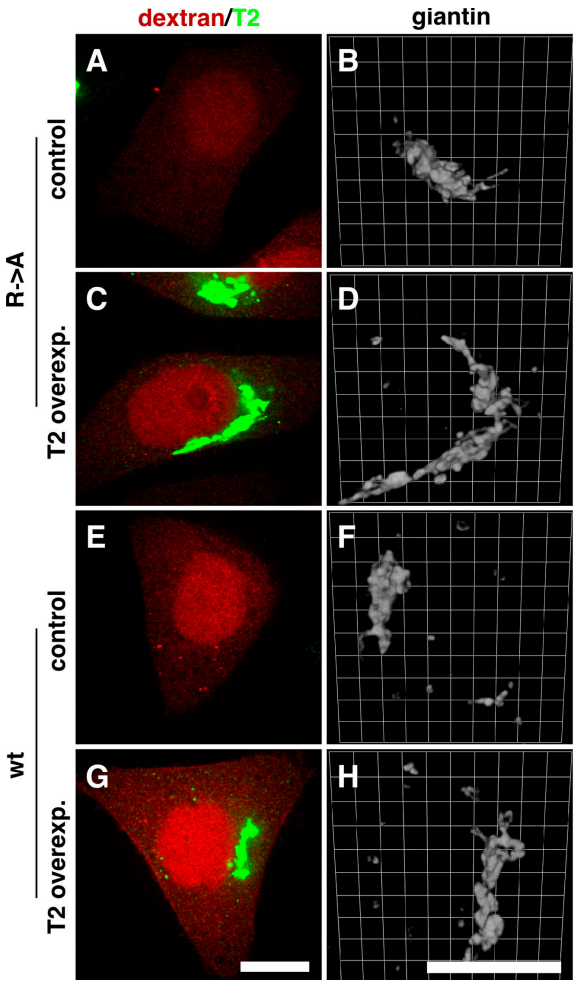

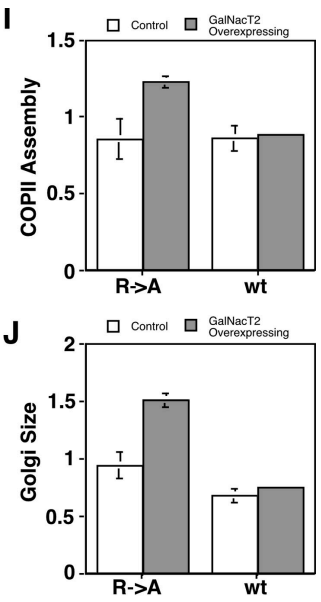

Figure 9. **Sar1p–GalNAcT2 interaction underlies Golgi size increase.** (A–H) HeLa cells stably transfected with T2-GFP were microinjected with the alanine-substituted control peptide (A–D; R→A) or the GalNAcT2 cytoplasmic domain peptide (E–H; wild type [wt]) at 1 mM in the presence of fluorescent dextran as a microinjection marker. After 45 min, the cells were paraformaldehyde-fixed and analyzed to reveal dextran and GFP fluorescence (red and green, respectively; A, C, E, and G), as well as giantin staining shown after 3D rendering (B, D, F, and H). Control cells were those that exhibited little or no detectable expression, whereas T2-GFP–overexpressing cells yielded strong Golgi and detectable ER staining. Bars, 10 μm. (I and J) COPII assembly (I) and Golgi size (J) were then quantified for all control or T2-GFP–overexpressing microinjected cells. Values are normalized means (± SD; $n = 2$; ≥12 cells each). Note that the GalNAcT2 peptide, but not the control peptide, blocked both the up-regulation of COPII assembly and the increase in Golgi size induced by T2-GFP.

Consistent with this, compared with cells in a control sample, we observed a twofold increase in Sec13 levels at exit sites in cells expressing VSVG-GFP, yet there was no significant difference in Golgi size induced by VSVG-GFP expression (Fig. 8, A–G). Using GM130 to measure Golgi size yielded identical results. Analysis of the data from single experiments on a cell-by-cell basis also supported these findings. In contrast to the case for T2-GFP, the COPII up-regulation induced by VSVG expression correlated poorly, if at all, with Golgi size (Fig. 8 H). Even under conditions of high-level VSVG-GFP expression induced by transient transfection (1.5-fold higher than T2-GFP based on total fluorescence per cell), there was no significant change in apparent Golgi size (1.0 ± 0.1–fold). If the COPII assembly increase induced by VSVG-GFP corresponded to increased input to the Golgi, as would be expected, then VSVG-GFP must have also induced a compensatory increase in output to account for the lack of change in Golgi size. Indeed, a transient Golgi size increase was previously observed coincident with a wave of VSVG passing through the Golgi (Aridor et al., 1999; Trucco et al., 2004), and we also observed increased Golgi size if we analyzed cells 20 min after releasing ER-accumulated VSVG-GFP using temperature shift (unpublished data). As further controls, we analyzed cells expressing the ER-localized protein Sec61-GFP (Voeltz et al., 2002) and the secreted protein albumin. Comparison of expressing to nonexpressing cells indicated that Sec61-GFP expression (at a level equal to T2-GFP based on total fluorescence per cell) altered neither COPII assembly nor Golgi size (Fig. S4 B) and that albumin expression modestly elevated COPII assembly but did not alter Golgi size (Fig. S4 C). In sum, these results suggest that COPII assembly can be induced by proteins rapidly exiting the ER and that, in the case of Golgi residents, this can lead to sustained changes in Golgi size.

If T2-GFP influences Golgi size via its interaction with the COPII coat, then interfering with this interaction should alter both COPII assembly and Golgi size. Consistent with this, it was shown in Fig. 6 in permeabilized cells that the GalNAcT2 cytoplasmic domain peptide, which binds Sar1p, blocks the up-regulation of COPII assembly induced by T2-GFP expression. Therefore, we microinjected this peptide or the alanine-substituted control peptide into nonexpressing and T2-GFP–expressing cells and, after 45 min, determined COPII assembly levels and Golgi size in cells marked by coinjected fluorescent dextran (Fig. 9, A–H). Microinjection itself led to an unexplained minimal increase in dissociated Golgi elements, but it did not alter steady-state changes in COPII assembly or Golgi size. That is, similar to noninjected cells, T2-GFP–overexpressing cells injected with the control peptide exhibited significant increases in both COPII assembly and Golgi size (Fig. 9, I and J, R→A).

In contrast, the GalNAcT2 peptide blocked both the COPII assembly increase and the Golgi size increase (Fig. 9, I and J, wt) strongly suggesting that the Golgi size increase evident in T2-GFP–expressing cells is a direct consequence of the COPII–Golgi protein interaction.

Discussion

COPII assembly was regulated by the availability of Golgi proteins in the ER that was due to, in the case of T2-GFP, a direct interaction between the Golgi protein cytoplasmic domain and Sar1p. Transient availability of Golgi proteins in the ER triggered transient COPII up-regulation, explaining the burst of Golgi growth that accompanies Golgi biogenesis from the ER. Further, when sustained, increased availability of Golgi proteins in the ER established a new, higher steady-state level of COPII assembly, and this accompanied a stable increase in Golgi size. Thus, our work shows for the first time that variable coat assembly regulated by compartment residents significantly impacts organelle homeostasis.

The binding of cargo to assembling coats is widely recognized to underlie the local enrichment of cargo at bud sites and, thus, sorting (Springer et al., 1999; Bonifacino and Glick, 2004). Less well recognized is that the capacity of cargo to bind coats influences coat assembly by increasing avidity of the coat for the membrane (Miller et al., 1991; Callus et al., 1996; Le Borgne and Hoflack, 1997; Aridor et al., 1999). GDP bound Sar1p interacted with GalNAcT2, suggesting that, as shown in the model (Fig. 10 A), increased GalNAcT2 in the ER membrane recruited more Sar1p-GDP and, after Sec12p-mediated GTP exchange, this led to increased formation of Sec23–Sec24 prebudding complexes. Whereas Sar1 is diffusely localized on the ER membrane, assembled COPII is not. A simple explanation is that lateral interactions between coat components accounts for the concentration of COPII into new and larger sites. That is, up-regulated Sar1 recruitment increases COPII components on the ER membrane, which in turn form new and larger clusters. It was very recently shown that secretory cargo influences formation of ER-to-Golgi tubular carriers (Simpson et al., 2006). It is unclear whether this is mechanistically related to ER exit site formation, but it may be that cargo-induced new and/or larger ER exit sites give rise to tubular carriers.

Cargo binding to the GDP form of Sar1p may be generally involved because, in addition to the dibasic-containing Golgi enzymes (Giraudo and Maccioni, 2003) and VSVG (Aridor et al., 2001), at least two SNAREs, Bet1p and Bos1p, also bind Sar1p-GDP (Springer and Schekman, 1998). Because all these proteins also bind Sar1p-GTP, an additional effect may be stabilization of Sar1p-GTP on the membrane. However, based on the failure of inhibition of GTP hydrolysis by Sar1p to induce COPII assembly up-regulation, Sar1p-GTP stabilization is not sufficient. Further, the best described cargo–COPII interactions involve binding sites on the Sec24p subunit (Miller et al., 2003; Mossessova et al., 2003), and SNARE binding at these sites stabilizes membrane binding of Sec23–Sec24p complex during multiple rounds of Sar1p-GTP hydrolysis (Sato and Nakano, 2005). Thus, cargo–coat interactions exert multilevel control of coat assembly.

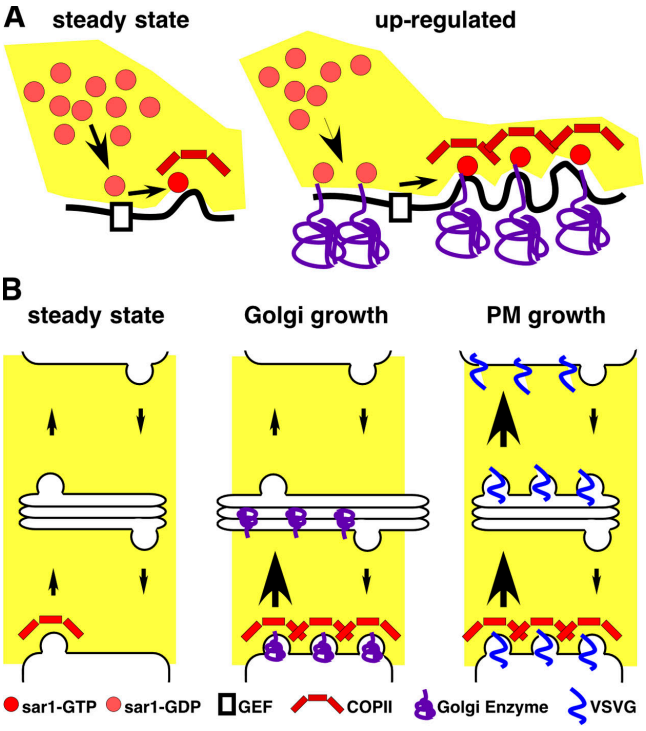

Figure 10. **Model depicting variable exit rate mechanism.** (A) COPII assembly is shown at steady state and after up-regulation by increased availability of Golgi residents in the ER membrane. The dibasic signal in the cytoplasmic domain of Golgi residents recruits more Sar1p-GDP to the ER membrane. After nucleotide exchange catalyzed by Sec12p and assembly of the prebudding complex, lateral interactions of the coat components leads to new and larger exit site formation. (B) Golgi input/output pathways are schematized before (steady state) or after either increased Golgi resident expression (Golgi growth) or increased plasma membrane protein expression (PM growth). Golgi residents up-regulate COPII assembly, leading to increased ER exit (denoted by larger arrow) and Golgi growth. Plasma membrane proteins up-regulate both ER exit and Golgi exit, leading to, at most, a transient increase in Golgi size.

Variable coat assembly regulated by compartment residents could profoundly impact organelle homeostasis (Fig. 10 B). Steady-state Golgi growth reflects the balance of all input and output reactions. Input reactions could be most sensitive to Golgi protein expression level, whereas output reactions might be most sensitive to the level of non-Golgi residents, such as proteins that rapidly recycle to the ER and newly synthesized proteins headed for distal compartments, including outside the cell, the cell surface, and lysosomes. If so, increased Golgi protein synthesis would cause increased Golgi growth because of increased input from the ER with a less dramatic change in exit from the Golgi. Because of the necessary presence of targeting and fusion factors accompanying the increased input from the ER, there is likely an increase in Golgi-to-ER recycling. An explanation for why this does not offset the size increase is that recycling involves less material and therefore less membrane. In contrast to Golgi protein synthesis, increased synthesis of plasma membrane proteins would cause a transient increase in Golgi size, as has been observed (Aridor et al., 1999; Trucco et al., 2004), but little lasting change in Golgi growth. That is, any increase in input to the Golgi from the ER would shortly thereafter be offset by a corresponding increase in exit from the

Golgi, possibly because of cargo–coat interactions at the TGN (Nishimura et al., 2002). Thus, homeostasis of endomembrane compartments might be partly determined by the level of compartment residents because of their influence on coat assembly and vesicle trafficking kinetics. Paralleling the sensitivity of COPII assembly to VSVG levels, assembly of the clathrin–AP2 complex is sensitive to transferrin receptor and mannose-6 phosphate receptor levels (Miller et al., 1991; Callus et al., 1996; Le Borgne and Hoflack, 1997). Future work may reveal that the cargo sensitivity of all coats extends to the level of compartment residents and that the sum of the consequent interactions establishes compartment size. Interestingly, other complex biological structures, such as the yeast spindle pole body, show size regulation via expression level (Bullitt et al., 1997; Elliott et al., 1999).

Variable coat assembly provides a straightforward way in which cells can respond to dramatic, reversible changes in the integrity of an organelle, such as the Golgi apparatus, and restore its original state. Conceivably, variable coat assembly also drives sustained changes in organelle size, such as those that occur during differentiation, by responding to coordinated changes in expression of organelle residents.

Materials and methods

Cell culture and immunofluorescence

NRK cells, HepG2 cells, HeLa cells, or HeLa cell lines stably expressing the GFP-tagged proteins GalNacT2 (T2-GFP), ts045-VSVG (VSVG-GFP), or GPP130 (GPP130-GFP) were maintained as described previously (Puri and Linstedt, 2003). BFA (Sigma-Aldrich) and H89 (Toronto Research) were used in media at 2.5 μg/ml and 100 μM, respectively. For transient transfections, HeLa cells were transfected with plasmids encoding GFP-tagged Sec13 (Hammond and Glick, 2000) using calcium phosphate or VSVG- or Sec61-GFP using Transfectol (GeneChoice). Immunofluorescence was performed as described previously (Puri and Linstedt, 2003). The antibodies and their dilutions were mouse anti-giantin at 1:100 (Linstedt and Hauri, 1993); rabbit anti-Sec13 at 1:500 (Kapetanovich et al., 2005); rabbit anti-Sec24p at 1:500 (provided by T.H. Lee, Carnegie Mellon University, Pittsburgh, PA); mouse anti–mannosidase II at 1:10,000 (Covance); rabbit anti-GM130 at 1:500 (Puthenveedu and Linstedt, 2001); FITC-conjugated anti–albumin at 1:100 (Biotrend); Cy5-labeled goat anti–mouse or anti–rabbit at 1:500 (Zymed Laboratories); and rhodamine-labeled goat anti–rabbit at 1:500 (Zymed Laboratories).

Image analysis

Microscopy was performed using a spinning disk confocal scan head equipped with three-line laser and independent excitation and emission filter wheels (PerkinElmer) and a 12-bit digital camera (Orca ER; Hamamatsu) mounted on a microscope (Axiovert 200; Carl Zeiss MicroImaging, Inc.) with a 100×, 1.4 NA apochromat oil-immersion objective (Carl Zeiss MicroImaging, Inc.). Single optical sections or sections at 0.3-μm spacing were acquired using ImagingSuite software (PerkinElmer). Individual experiments were performed with identical laser output levels, exposure times, and scaling. At least six representative fields, each containing 3–5 cells, were taken. Total fluorescence of Sec13 at peripheral sites was quantified using ImageJ on single optical sections as follows. For each experiment, a single fixed threshold was manually chosen (based on comparison to the original gray-scale images) and applied to all images. Individual cells were then selected with the free-hand tool, and the total above-threshold fluorescence was determined using either the analyze particles or measure functions. For quantification of Golgi size, the analyze particles function was used after thresholding to yield, on a per-cell basis, the sum of each section's Golgi area as determined by giantin or GM130 staining. Cell volume was estimated by summing the area in each section outlined manually based on the diffuse background staining of Sec13. To allow direct comparison of distinct experiments given small changes in staining intensity, COPII assembly and Golgi size values were normalized by dividing by the mean values of the entire dataset for a given experiment. To compare expression level of GFP constructs, single optical sections were acquired using identical settings and the 12-bit images were background subtracted using a fixed value (202). Means of the total fluorescence per cell were compared (>10 cells each). Live imaging was performed 2 d after transfection in Optimem (Invitrogen) containing 10% fetal bovine serum on a 37°C stage using 300-ms exposures every 2 min. For each time point, fluorescence intensity in objects was determined as just described. These values were then adjusted to correct for the slight rate of photobleaching based on the photobleaching rate of an identically captured movie for a control cell outside of the dataset. The values for a given cell were then normalized by dividing each by the mean value of the last five time points for that cell. This allowed direct comparison of distinct cells. Neither the correction nor the normalization altered the pattern of fluorescence changes.

Permeabilized cell assays

The morphological permeabilized cell COPII assembly assay was performed as described previously (Kapetanovich et al., 2005). NRK cells at 70% confluence on 12-mm glass coverslips were treated with BFA for 30 min, washed 3 × 0.5 ml with cold DME, and washed 2 × 0.5 ml with cold KOAc buffer (115 mM KOAc, 2.5 mM MgOAc, 25 mM Hepes, pH 7.2, and 1 mM dithiothreitol). The washed cells were permeabilized 6 min at RT in 0.5 ml 0.03 mg/ml digitonin in KOAc buffer followed by 3 × 0.5 ml washes in cold KOAc buffer. After transfer to parafilm, the coverslips were incubated at 37°C for 10 min in 50 μl KOAc buffer containing either rabbit liver cytosol, at the indicated concentrations, or purified yeast Sar1p (1 μg/ml), Sec23p–Sec24p (3 μg/ml), and Sec13p–Sec31p (7 μg/ml). Where indicated, each reaction also contained 500 μM GTPγS and an ATP regeneration system (0.5 mM ATP, 0.5 mM UTP, 50 μM GTP, 5 mM creatine phosphate, 25 μg/ml creatine phosphokinase, 0.05 mM EGTA, and 0.5 mM $MgCl_2$). The coverslips were then washed in cold KOAc buffer and fixed and stained as described. The morphological assay was slightly modified for the peptide inhibition experiments. T2-GFP cells were used instead of NRK and, before use, the cytosol was preincubated at 4°C 1 h in 20-μl reactions containing 0.2 mg cytosol, 500 μM GTPγS, the ATP regeneration system, 1 mM PMSF, and synthetic peptides (see Peptide binding) at the indicated concentrations.

The immunoblot-based assay was essentially the same except that cells were grown in 35-mm dishes and volumes were scaled accordingly. Instead of fixation, the washed cells were scraped into lysis buffer (1% TX-100, 2 mM EDTA, 50 mM Tris, pH 8.0, 1 mM PMSF, and 150 mM NaCl) and incubated on ice for 10 min with vortexing followed by centrifugation at 14,000 rpm for 5 min. The cleared lysate was precipitated using trichloroacetic acid and analyzed by immunoblotting (Linstedt and Hauri, 1993) using enhanced chemiluminescence (Pierce Chemical Co.) with acquisition by the LAS-3000 imaging system (Fujifilm). Antibodies used were rabbit anti-Sec13 at 1:1,000 (Kapetanovich et al., 2005), rabbit anti-GPP130 at 1:1,000 (Puri et al., 2002), and peroxidase-conjugated anti–rabbit at 1:5,000 (Bio-Rad Laboratories).

Peptide binding

Synthetic peptides (MRRRSRC and MAAASAC) were purchased from GeneScript and coupled via the added C-terminal cysteine residue to Sepharose 6B beads according to previous work (Dominguez et al., 1998; Giraudo and Maccioni, 2003) and manufacturer instructions (GE Healthcare) in reactions containing 100 μl 14 mg/ml peptide, 500 μl beads, and 600 μl coupling buffer (50 mM Tris, pH 7.3, and 0.5 M NaCl). Coupling efficiency was determined by the measuring 2-thiopyridone release at 343 nm. The beads (14-μl aliquots) were then blocked by a 40-min 4°C incubation in 0.5 ml 5 mM β-mercaptoethanol, 50 mM NaOAc, 0.5 M NaCl, pH 4.5, followed by washing and a 2-h 4°C incubation in binding buffer (20 mM Hepes, pH 7.2, 250 mM sorbitol, 70 mM KOAc, 1 mM Mg[OAc]2, and 1 mg/ml bovine serum albumin). For binding experiments, 0.5 μg Sar1p was preincubated for 30 min at 4°C in the presence or absence of 500 μM GTPγS in a total volume of 14 μl binding buffer. To this was added 16 μl buffer containing 7 μl beads containing 5 nmoles of peptide for 1 h at 4°C. The beads were washed 4 × 500 μl for 1 min each with binding buffer lacking albumin and analyzed for Sar1p recovery by immunoblot as described in the previous paragraph using rabbit anti-Sar1p antibody at 1:2,000.

Microinjection

The MRRRSRC or MAAASAC peptides were microinjected into T2-GFP cells at 1 mM in water containing 0.25 mg/ml Alexa 568–conjugated

dextran (Invitrogen) using a FemtoJet system with InjectMan-NI2 micromanipulator (Brinkman). The injected cells were maintained at 37°C in Optimem containing 10% serum for 45 min followed by analysis of COPII assembly using anti-Sec13 and Golgi size using anti-giantin as described in Image analysis.

Online supplemental material

Fig. S1 shows up-regulation of COPII assembly at exit sites using representative frames and quantified data from live imaging experiments in which Sec13-GFP was visualized in control cells or upon BFA treatment. Fig. S2 and Fig. S3 show the specific inhibition of T2-GFP–induced COPII up-regulation by addition of the GalNAcT2 cytoplasmic domain peptide to the permeabilized cell assay. Representative images are presented in Fig. S2; total quantified Sec13 fluorescence is presented in Fig. 6; and quantification of number, size, and intensity of fluorescent objects (ER exit sites) is presented in Fig. S3. Fig. S4 shows that Golgi size is increased by overexpression of the Golgi protein GPP130 but not by overexpression of the ER protein Sec61 or the secreted protein albumin using representative images and quantified data. Online supplemental material is available at http://www.jcb.org/cgi/content/full/jcb.200604058/DC1.

We thank Dr. T.H. Lee for COPII reagents and expert advice, the Linstedt laboratory (especially Dr. M.A. Puthenveedu for invaluable suggestions and T. Feinstein for help in generating stable cell lines), and Russell Schwartz for modeling work that sparked interest in this project.

This work was supported by National Institutes of Health grant GM-56779 to A.D. Linstedt.

Submitted: 12 April 2006
Accepted: 30 May 2006

References

Antonny, B., D. Madden, S. Hamamoto, L. Orci, and R. Schekman. 2001. Dynamics of the COPII coat with GTP and stable analogues. *Nat. Cell Biol.* 3:531–537.

Aridor, M., and L.M. Traub. 2002. Cargo selection in vesicular transport: the making and breaking of a coat. *Traffic.* 3:537–546.

Aridor, M., J. Weissman, S. Bannykh, C. Nuoffer, and W.E. Balch. 1998. Cargo selection by the COPII budding machinery during export from the ER. *J. Cell Biol.* 141:61–70.

Aridor, M., S.I. Bannykh, T. Rowe, and W.E. Balch. 1999. Cargo can modulate COPII vesicle formation from the endoplasmic reticulum. *J. Biol. Chem.* 274:4389–4399.

Aridor, M., K.N. Fish, S. Bannykh, J. Weissman, T.H. Roberts, J. Lippincott-Schwartz, and W.E. Balch. 2001. The Sar1 GTPase coordinates biosynthetic cargo selection with endoplasmic reticulum export site assembly. *J. Cell Biol.* 152:213–229.

Bednarek, S.Y., M. Ravazzola, M. Hosobuchi, M. Amherdt, A. Perrelet, R. Schekman, and L. Orci. 1995. COPI- and COPII-coated vesicles bud directly from the endoplasmic reticulum in yeast. *Cell.* 83:1183–1196.

Bonifacino, J.S., and B.S. Glick. 2004. The mechanisms of vesicle budding and fusion. *Cell.* 116:153–166.

Buccione, R., S. Bannykh, I. Santone, M. Baldassarre, F. Facchiano, Y. Bozzi, G. Di Tullio, A. Mironov, A. Luini, and M.A. De Matteis. 1996. Regulation of constitutive exocytic transport by membrane receptors. A biochemical and morphometric study. *J. Biol. Chem.* 271:3523–3533.

Bullitt, E., M.P. Rout, J.V. Kilmartin, and C.W. Akey. 1997. The yeast spindle pole body is assembled around a central crystal of Spc42p. *Cell.* 89:1077–1086.

Callus, B.A., B.J. Iacopetta, L.C. Kuhn, and E.H. Morgan. 1996. Effects of overexpression of the transferrin receptor on the rates of transferrin recycling and uptake of non-transferrin-bound iron. *Eur. J. Biochem.* 238:463–469.

Colanzi, A., C. Suetterlin, and V. Malhotra. 2003. Cell-cycle-specific Golgi fragmentation: how and why? *Curr. Opin. Cell Biol.* 15:462–467.

Dominguez, M., K. Dejgaard, J. Fullekrug, S. Dahan, A. Fazel, J.P. Paccaud, D.Y. Thomas, J.J. Bergeron, and T. Nilsson. 1998. gp25L/emp24/p24 protein family members of the cis-Golgi network bind both COP I and II coatomer. *J. Cell Biol.* 140:751–765.

Donaldson, J.G., D. Finazzi, and R.D. Klausner. 1992. Brefeldin A inhibits Golgi membrane-catalysed exchange of guanine nucleotide onto ARF protein. *Nature.* 360:350–352.

Elliott, S., M. Knop, G. Schlenstedt, and E. Schiebel. 1999. Spc29p is a component of the Spc110p subcomplex and is essential for spindle pole body duplication. *Proc. Natl. Acad. Sci. USA.* 96:6205–6210.

Forster, R., M. Weiss, T. Zimmermann, E.G. Reynaud, F. Verissimo, D.J. Stephens, and R. Pepperkok. 2006. Secretory cargo regulates the turnover of COPII subunits at single ER exit sites. *Curr. Biol.* 16:173–179.

Futai, E., S. Hamamoto, L. Orci, and R. Schekman. 2004. GTP/GDP exchange by Sec12p enables COPII vesicle bud formation on synthetic liposomes. *EMBO J.* 23:4146–4155.

Giraudo, C.G., and H.J. Maccioni. 2003. Endoplasmic reticulum export of glycosyltransferases depends on interaction of a cytoplasmic dibasic motif with Sar1. *Mol. Biol. Cell.* 14:3753–3766.

Goldberg, J. 2000. Decoding of sorting signals by coatomer through a GTPase switch in the COPI coat complex. *Cell.* 100:671–679.

Hammond, A.T., and B.S. Glick. 2000. Dynamics of transitional endoplasmic reticulum sites in vertebrate cells. *Mol. Biol. Cell.* 11:3013–3030.

Helms, J.B., and J.E. Rothman. 1992. Inhibition by brefeldin A of a Golgi membrane enzyme that catalyses exchange of guanine nucleotide bound to ARF. *Nature.* 360:352–354.

Ikonomov, O.C., D. Sbrissa, and A. Shisheva. 2001. Mammalian cell morphology and endocytic membrane homeostasis require enzymatically active phosphoinositide 5-kinase PIKfyve. *J. Biol. Chem.* 276:26141–26147.

Kapetanovich, L., C. Baughman, and T.H. Lee. 2005. Nm23H2 facilitates coat protein complex II assembly and endoplasmic reticulum export in mammalian cells. *Mol. Biol. Cell.* 16:835–848.

Knaapen, M.W., B.C. Vrolijk, and A.C. Wenink. 1997. Ultrastructural changes of the myocardium in the embryonic rat heart. *Anat. Rec.* 248:233–241.

Kuehn, M.J., J.M. Herrmann, and R. Schekman. 1998. COPII-cargo interactions direct protein sorting into ER-derived transport vesicles. *Nature.* 391:187–190.

Le Borgne, R., and B. Hoflack. 1997. Mannose 6-phosphate receptors regulate the formation of clathrin-coated vesicles in the TGN. *J. Cell Biol.* 137:335–345.

Lee, T.H., and A.D. Linstedt. 1999. Osmotically induced cell volume changes alter anterograde and retrograde transport, Golgi structure, and COPI dissociation. *Mol. Biol. Cell.* 10:1445–1462.

Lee, T.H., and A.D. Linstedt. 2000. Potential role for protein kinases in regulation of bidirectional endoplasmic reticulum-to-Golgi transport revealed by protein kinase inhibitor H89. *Mol. Biol. Cell.* 11:2577–2590.

Linstedt, A.D., and H.P. Hauri. 1993. Giantin, a novel conserved Golgi membrane protein containing a cytoplasmic domain of at least 350 kDa. *Mol. Biol. Cell.* 4:679–693.

Linstedt, A.D., A. Mehta, J. Suhan, H. Reggio, and H.P. Hauri. 1997. Sequence and overexpression of GPP130/GIMPc: evidence for saturable pH-sensitive targeting of a type II early Golgi membrane protein. *Mol. Biol. Cell.* 8:1073–1087.

Lu, Z., D. Joseph, E. Bugnard, K.J. Zaal, and E. Ralston. 2001. Golgi complex reorganization during muscle differentiation: visualization in living cells and mechanism. *Mol. Biol. Cell.* 12:795–808.

Matsuoka, K., L. Orci, M. Amherdt, S.Y. Bednarek, S. Hamamoto, R. Schekman, and T. Yeung. 1998. COPII-coated vesicle formation reconstituted with purified coat proteins and chemically defined liposomes. *Cell.* 93:263–275.

Miller, E.A., T.H. Beilharz, P.N. Malkus, M.C. Lee, S. Hamamoto, L. Orci, and R. Schekman. 2003. Multiple cargo binding sites on the COPII subunit Sec24p ensure capture of diverse membrane proteins into transport vesicles. *Cell.* 114:497–509.

Miller, K., M. Shipman, I.S. Trowbridge, and C.R. Hopkins. 1991. Transferrin receptors promote the formation of clathrin lattices. *Cell.* 65:621–632.

Mossessova, E., L.C. Bickford, and J. Goldberg. 2003. SNARE selectivity of the COPII coat. *Cell.* 114:483–495.

Nishimura, N., and W.E. Balch. 1997. A di-acidic signal required for selective export from the endoplasmic reticulum. *Science.* 277:556–558.

Nishimura, N., H. Plutner, K. Hahn, and W.E. Balch. 2002. The delta subunit of AP-3 is required for efficient transport of VSV-G from the trans-Golgi network to the cell surface. *Proc. Natl. Acad. Sci. USA.* 99:6755–6760.

Orci, L., A. Perrelet, M. Ravazzola, F.T. Wieland, R. Schekman, and J.E. Rothman. 1993. "BFA bodies": a subcompartment of the endoplasmic reticulum. *Proc. Natl. Acad. Sci. USA.* 90:11089–11093.

Puri, S., and A.D. Linstedt. 2003. Capacity of the Golgi apparatus for biogenesis from the endoplasmic reticulum. *Mol. Biol. Cell.* 14:5011–5018.

Puri, S., C. Bachert, C.J. Fimmel, and A.D. Linstedt. 2002. Cycling of early Golgi proteins via the cell surface and endosomes upon lumenal pH disruption. *Traffic.* 3:641–653.

Puthenveedu, M.A., and A.D. Linstedt. 2001. Evidence that Golgi structure depends on a p115 activity that is independent of the vesicle tether components giantin and GM130. *J. Cell Biol.* 155:227–238.

Sato, K., and A. Nakano. 2005. Dissection of COPII subunit-cargo assembly and disassembly kinetics during Sar1p-GTP hydrolysis. *Nat. Struct. Mol. Biol.* 12:167–174.

Simpson, J.C., T. Nilsson, and R. Pepperkok. 2006. Biogenesis of tubular ER-to-Golgi transport intermediates. *Mol. Biol. Cell.* 17:723–737.

Springer, S., and R. Schekman. 1998. Nucleation of COPII vesicular coat complex by endoplasmic reticulum to Golgi vesicle SNAREs. *Science.* 281:698–700.

Springer, S., A. Spang, and R. Schekman. 1999. A primer on vesicle budding. *Cell.* 97:145–148.

Trucco, A., R.S. Polishchuk, O. Martella, A. Di Pentima, A. Fusella, D. Di Giandomenico, E. San Pietro, G.V. Beznoussenko, E.V. Polishchuk, M. Baldassarre, et al. 2004. Secretory traffic triggers the formation of tubular continuities across Golgi sub-compartments. *Nat. Cell Biol.* 6:1071–1081.

Voeltz, G.K., M.M. Rolls, and T.A. Rapoport. 2002. Structural organization of the endoplasmic reticulum. *EMBO Rep.* 3:944–950.

Ward, T.H., R.S. Polishchuk, S. Caplan, K. Hirschberg, and J. Lippincott-Schwartz. 2001. Maintenance of Golgi structure and function depends on the integrity of ER export. *J. Cell Biol.* 155:557–570.

Yoshihisa, T., C. Barlowe, and R. Schekman. 1993. Requirement for a GTPase-activating protein in vesicle budding from the endoplasmic reticulum. *Science.* 259:1466–1468.

Yu, W., L.E. O'Brien, F. Wang, H. Bourne, K.E. Mostov, and M.M. Zegers. 2003. Hepatocyte growth factor switches orientation of polarity and mode of movement during morphogenesis of multicellular epithelial structures. *Mol. Biol. Cell.* 14:748–763.